3^a Reunión Presencial del
Proyecto VMGRID
(ATLAS TIER2 ESPAÑA)
Madrid, Junio 13-14, 2019

UNIVERSIDAD AUTONOMA DE MADRID

ATLAS

User Support and Analysis at UAM:

Measurement of inclusive isolated-photon cross sections at $\sqrt{s} = 13$ TeV using 36 fb^{-1} and beyond

J del Peso & C Glasman
Universidad Autónoma de Madrid

Contents:

- Reminder
- Status
- Next steps

Reminder: Prompt-photon production: motivation

- Measurements of inclusive isolated-photon cross sections allow
  - → tests of pQCD
  - → constraints on the proton PDFs
  - → constraints on background to new particles decaying into photons

- Previous studies:

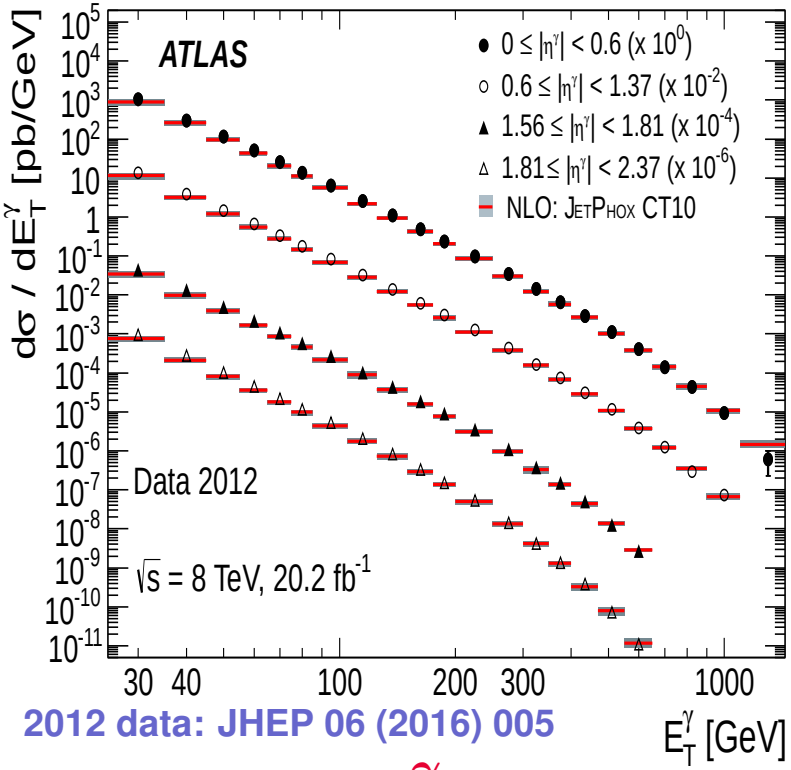

2012 data: JHEP 06 (2016) 005

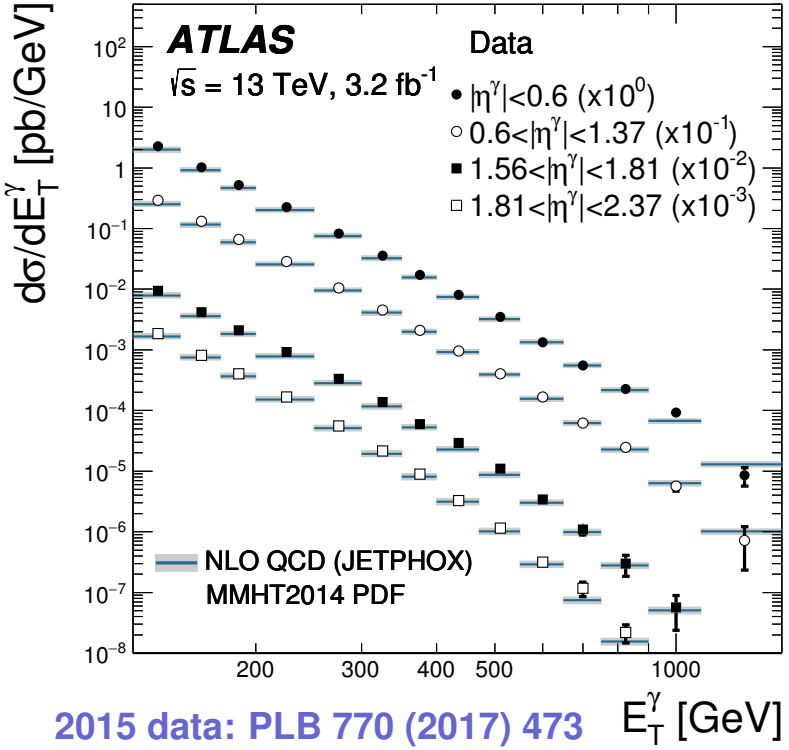

2015 data: PLB 770 (2017) 473

⇒ With 2015+2016 data, a higher E_T^γ reach is possible
  - → the region where the measurements are dominated by the systematic uncertainties is extended significantly towards higher E_T^γ

Reminder: Prompt photons in pp collisions at LHC

- Prompt photons in pp collisions ($pp \longrightarrow \gamma(+\mathrm{jet}) + \mathrm{X}$) are produced via two mechanisms:

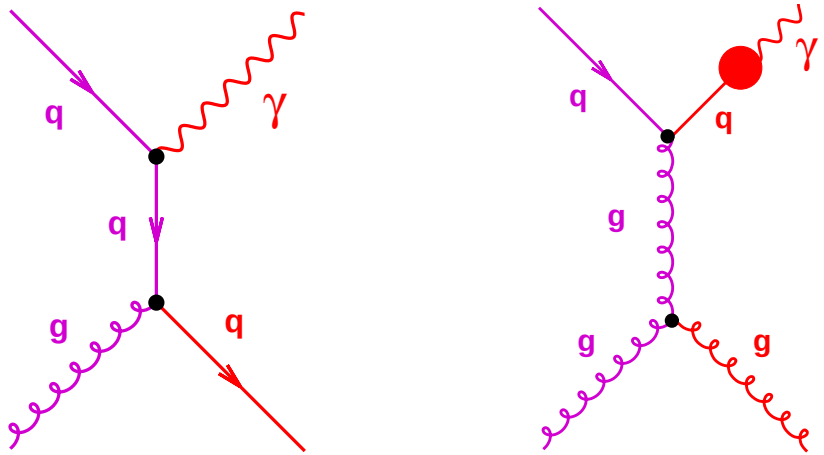

direct-photon (DP) fragmentation (F)

- In addition to prompt photons, photons are produced copiously inside jets (eg, π^0 decays)
  $\Rightarrow$ it is essential to require **isolation** to study prompt photons in hadron colliders
- This is achieved by requiring $E_{\mathrm{T}}^{\mathrm{iso}} \equiv \sum_i E_T^i < E_T^{\mathrm{max}}$, with the sum over the particles (except the photon!) inside a cone of radius R centered on the photon in the $\eta - \phi$ plane
- The isolation requirement suppresses mostly the contribution of photons inside jets and the fragmentation contribution

Reminder: Details on data

- **Data samples:**
  - → 2015; periods D-J ($\mathcal{L} = 3.21 \pm 0.07$ fb^{-1})
    (GRL: data15_13TeV.periodAllYear_DetStatus-v79-repro20-02_DQDefects-00-02-02_PHYS_StandardGRL_All_Good 25ns.xml)
  - → 2016; periods A-K ($\mathcal{L} = 32.9 \pm 0.7$ fb^{-1})
    (GRL: data16_13TeV.periodAllYear_DetStatus-v88-pro20-21_DQDefects-00-02-04_PHYS_StandardGRL_All_Good 25ns.xml)
- **Main steps of analysis of data:**
  - Data quality
  - Trigger selection
  - Photon calibration, identification and selection
  - Isolation computation and correction

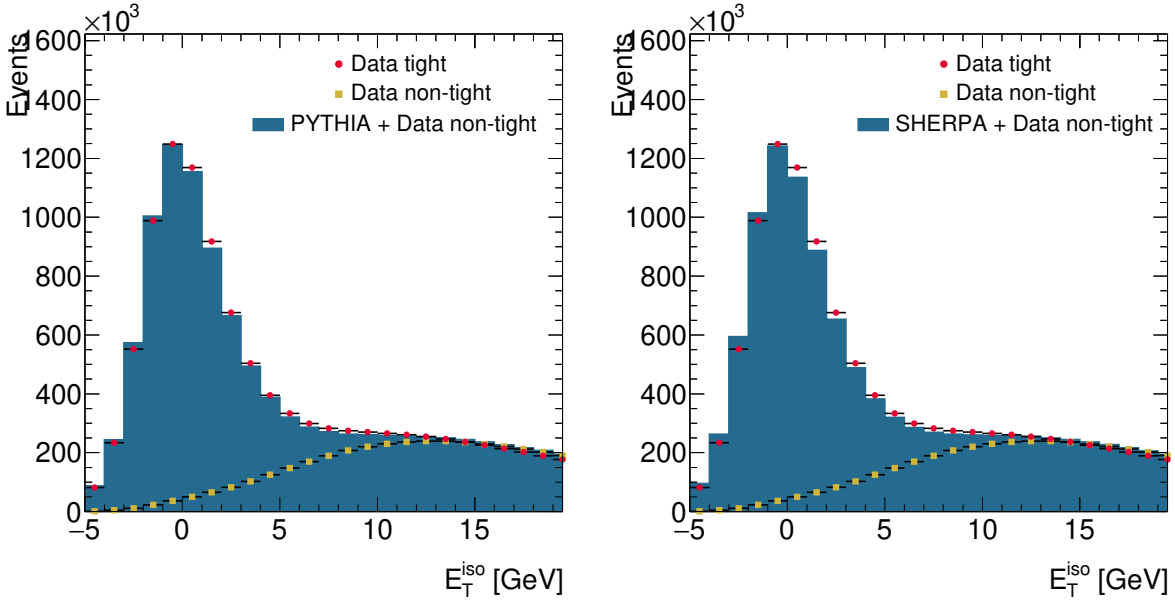

Reminder: Details on Monte Carlo simulations

- **Monte Carlo samples of PYTHIA and SHERPA are used to**
  - → **study the characteristics of signal events**
  - → **determine unfolding correction factors**
  - → **estimate hadronisation corrections to the NLO QCD calculations**
- **Main steps of analysis of Monte Carlo simulations (reco and truth levels):**
  - — **Photon calibration, identification and selection similar to data**
  - — **Isolation computation and correction similar to data**
  - — **Additional corrections due to mismatch between data and Monte Carlo**
  - — **Definition of phase space for measurement done at truth level**

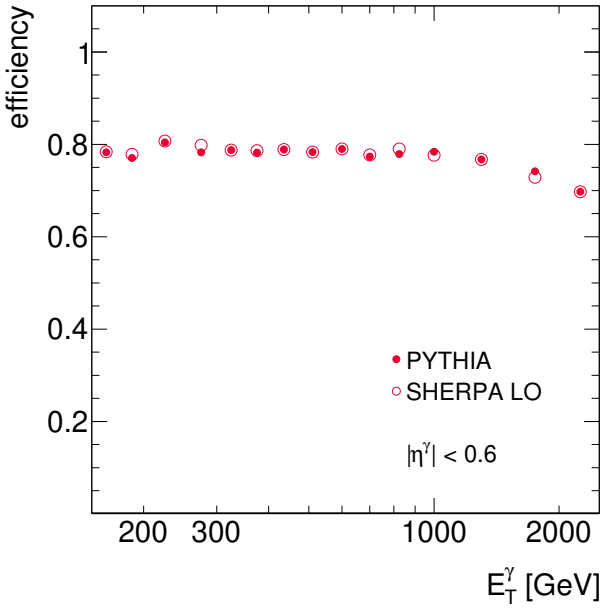

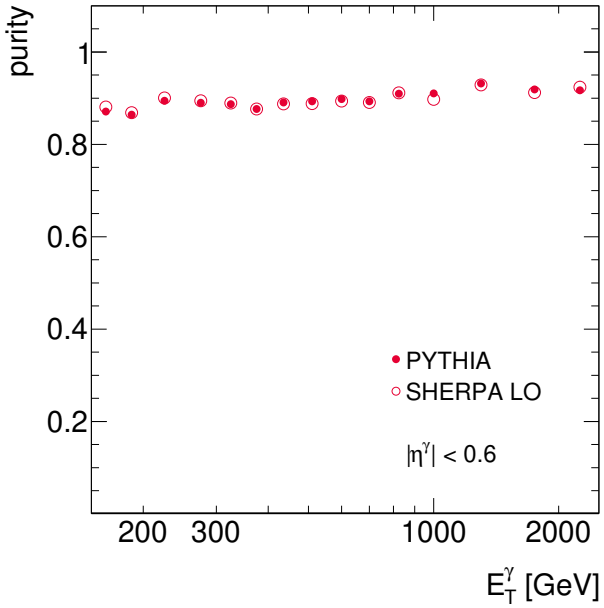

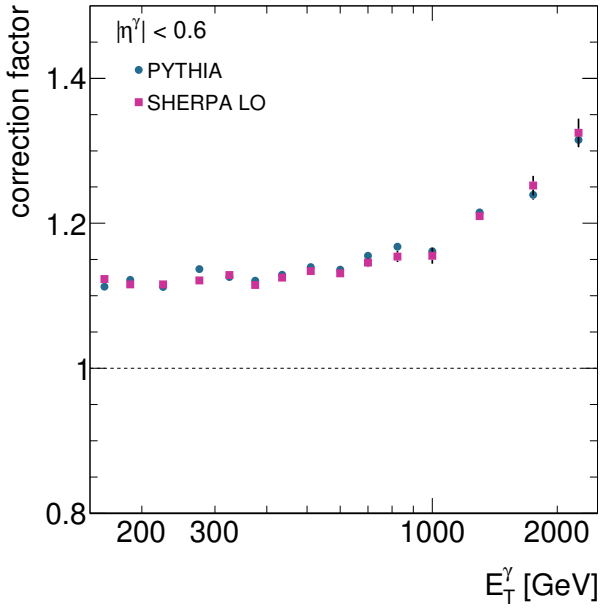

Reminder: Next-to-leading-order QCD calculations

- **JETPHOX:** full fixed-order NLO pQCD predictions for direct and fragmentation contributions; fixed-cone isolation
  - → scale: $\mu_R = \mu_F = \mu_f = E_{\rm T}^{\gamma}$
  - → PDF: MMHT2014 (also CT14, ABMP16, HERAPDF2.0, NNPDF3.0)
  - → $\alpha_{\rm s} = 0.120$ (MMHT2014); $\alpha_{\rm em} = 1/137.036$
  - → non-perturbative corrections for hadronisation and underlying event needed (computed using PYTHIA samples, $< 1\%$)

- **NLO SHERPA:** parton-level calculations for $\gamma + 1, 2$ jets at NLO and $\gamma + 3, 4$ jets at LO supplemented with parton shower; only direct contribution; hybrid-cone isolation
  - → scale: dynamic scale setting
  - → PDF: NNPDF3.0
  - → $\alpha_{\rm s} = 0.118$; $\alpha_{\rm em} = 1/137.036$
  - → predictions at particle level

- **Theoretical uncertainties:** higher orders (dominant), PDF-induced uncertainty, uncertainty on $\alpha_{\rm s}$ and hadronisation+UE corrections (JETPHOX)

JETPHOX (S. Catani et al, JHEP 0205 (2002) 028) NLO SHERPA (T. Gleisberg et al, JHEP 0902 (2009) 007)

New: Next-to-next-to-leading-order QCD calculations

- **Photon production at NNLO QCD accuracy:**
  - → fixed-order NNLO pQCD predictions for direct contributions; hybrid-cone isolation (loose Frixione plus fixed-cone isolation)
  - → NNLO corrections include
    - – two-loop corrections to photon-plus-one-parton production
    - – virtual corrections to photon-plus-two-parton production
    - – tree-level photon-plus-three-parton production
  - → scale: $\mu_R = \mu_F = E_{\rm T}^{\gamma}$
  - → PDF: NNPDF3.1
  - → $\alpha_{\rm s} = 0.118$; $\alpha_{\rm em} = 1/132.232$

- **Theoretical uncertainties:**
  - → higher orders and hadronisation+UE corrections ($\approx 1\%$) only

X Chen et al, arXiv:1904.01044

Isolated-photon production analysis

- **Status of analysis:**
  - → Analysis of 2015+2016 data completed at the end of March 2018
  - → EdBoard requested on plenary SM meeting on March 22nd, 2018
  - → EdBoard formed in April 2018
  - → Several meetings with EdBoard followed
  - → Analysis approved by SM group convenors and EdBoard on September 27th, 2018
  - → Internal note: ATL-COM-PHYS-2018-226 (https://cds.cern.ch/record/2308262)
  - → Draft: https://cds.cern.ch/record/2650055
  - → First circulation on February 28th, 2019: https://cds.cern.ch/record/2665024
    - ⋆ ATLAS weekly on March 5th, 2019
    - ⋆ 8 comments received
    - ⋆ PAM on March 20th, 2019
  - → While working on second draft, the NNLO calculations were published (see previous slide) and were incorporated into the draft (slight delay)
  - → Current status:
    - ⋆ EdBoard approved new draft on June 6th and comments in CDS replied
    - ⋆ Language editor assigned and process started on June 6th

Figures in paper

- **Systematic uncertainties:**

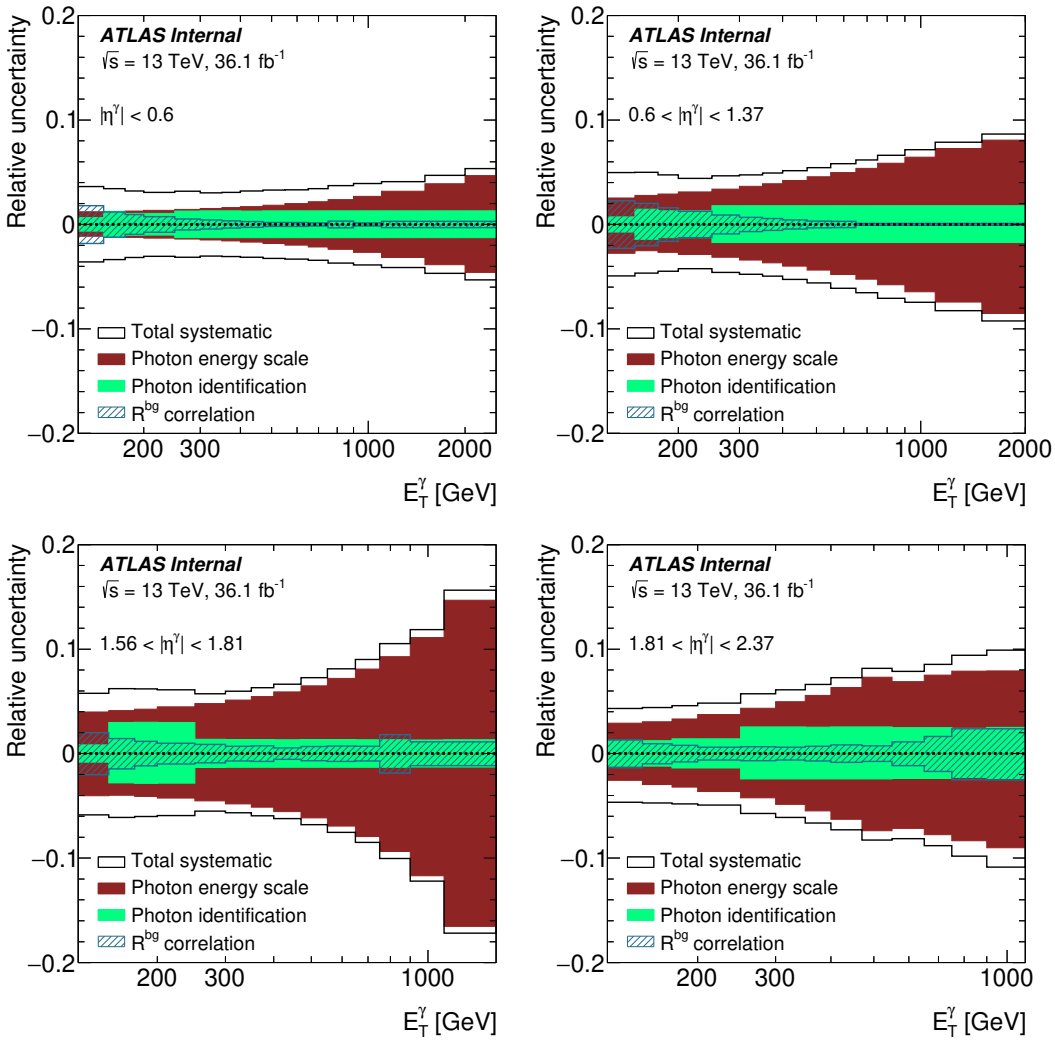

Figure 1: The relative total systematic uncertainty (white areas), the relative uncertainty due to the photon energy scale (brown areas), the relative uncertainty due to the photon identification efficiency (green areas) and the relative uncertainty due to R^{bg} (blue hatched areas) as functions of E_T^γ in different $|\eta^\gamma|$ regions.

Figures in paper

- **Experimental uncertainties:**

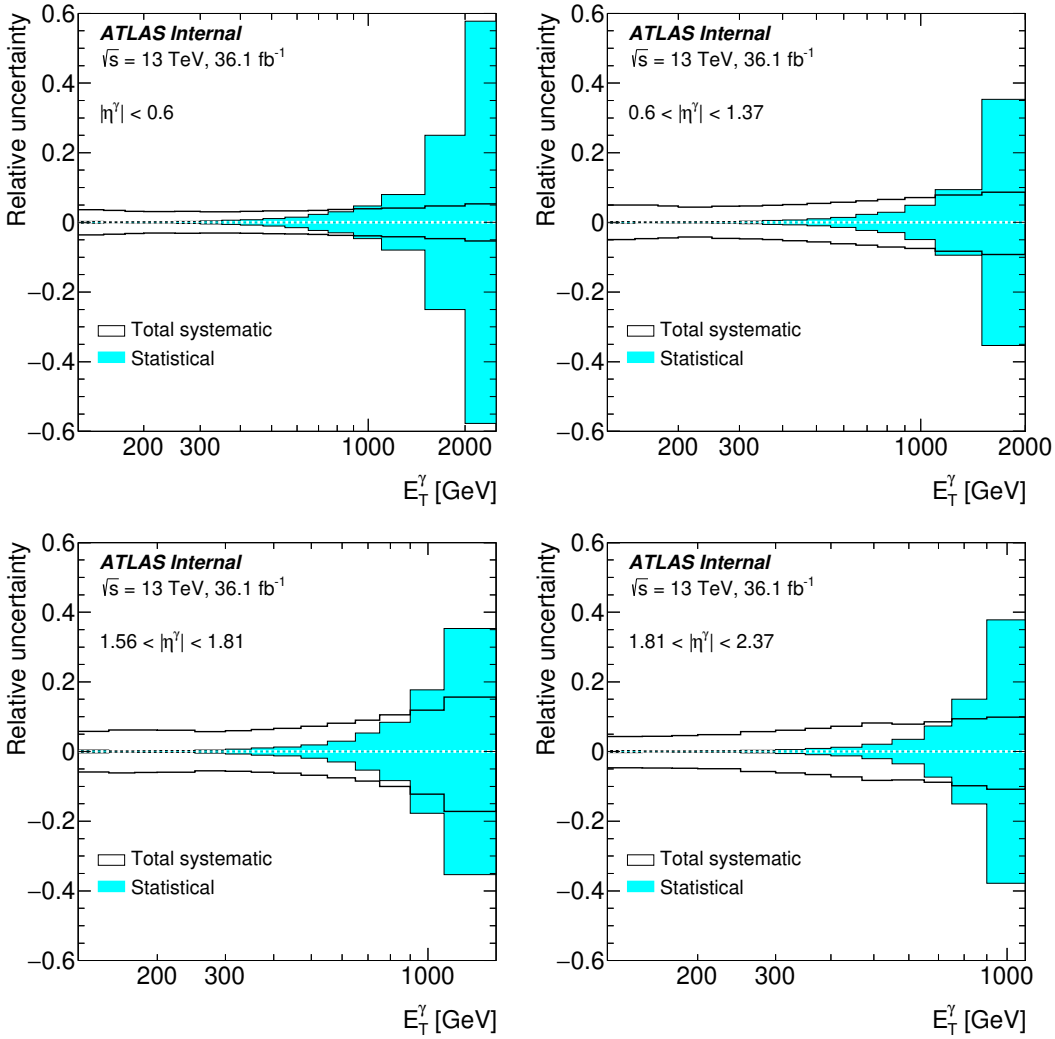

Figure 2: The relative total systematic uncertainty (white areas) and the relative statistical uncertainty from the data (cyan areas) as functions of E_{T}^{γ} in different $|\eta^{\gamma}|$ regions.

Figures in paper

- **Theoretical uncertainties:**

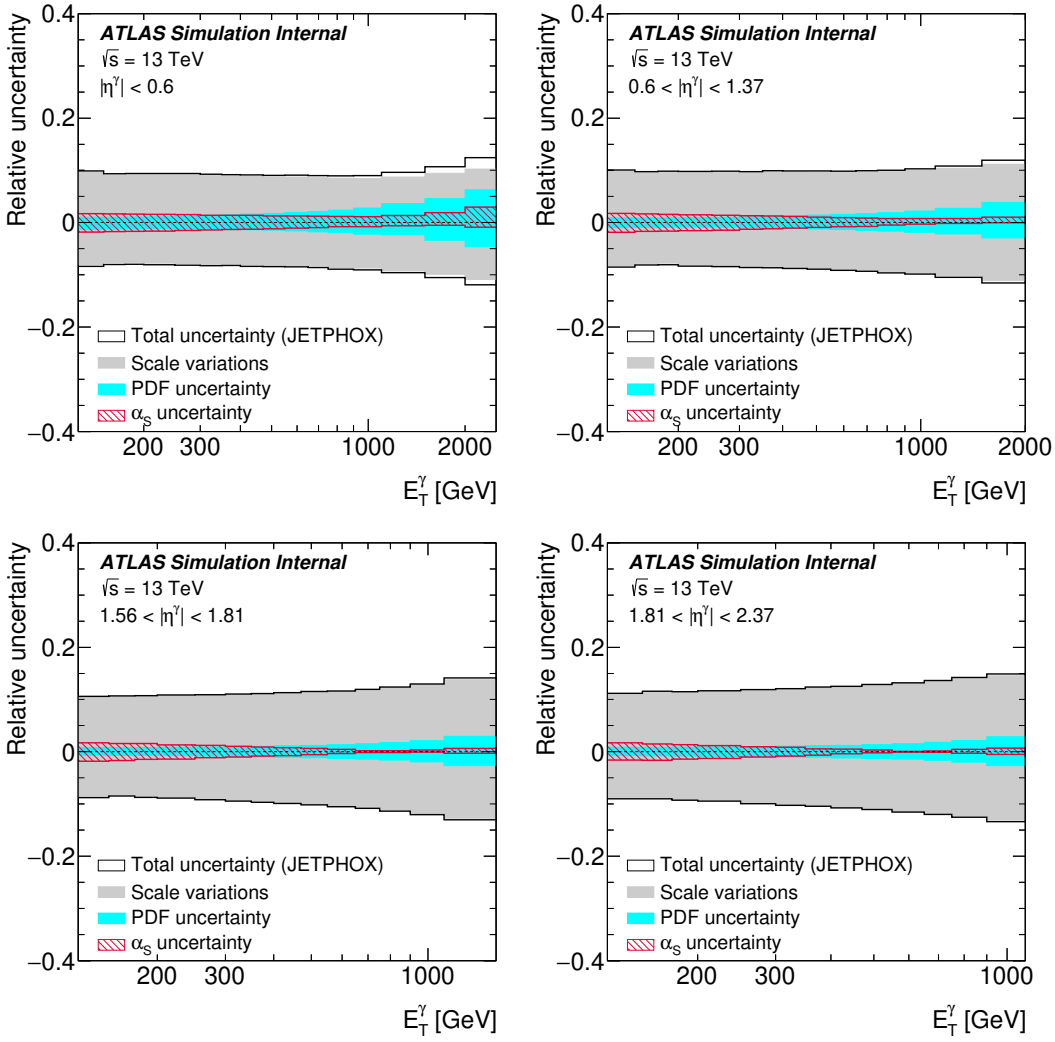

Figure 3: The relative total theoretical uncertainty (white areas) in the JETPHOX predictions as a function of E_{T}^{γ} in different regions of $|\eta^{\gamma}|$. The uncertainty from the scale variations (grey areas), the uncertainty from the PDFs (cyan areas) and the uncertainty from the value of α_{s} (red hatched areas) are also included.

Figures in paper

- **Theoretical uncertainties:**

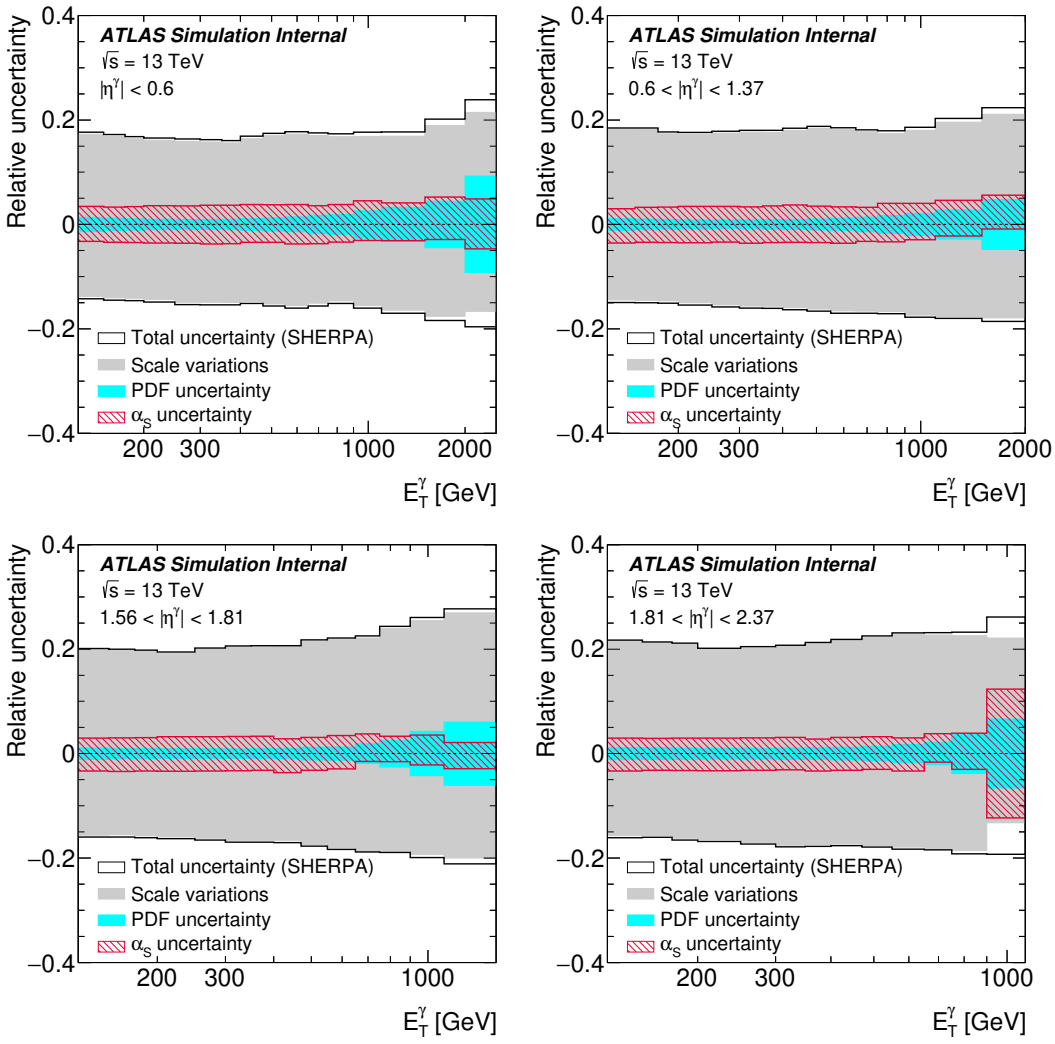

Figure 4: The relative total theoretical uncertainty (white areas) in the SHERPA 2.2.2 predictions as a function of E_{T}^{γ} in different regions of $|\eta^{\gamma}|$. The uncertainty from the scale variations (grey areas), the uncertainty from the PDFs (cyan areas) and the uncertainty from the value of α_{s} (red hatched areas) are also included.

Figures in paper

- **Theoretical uncertainties:**

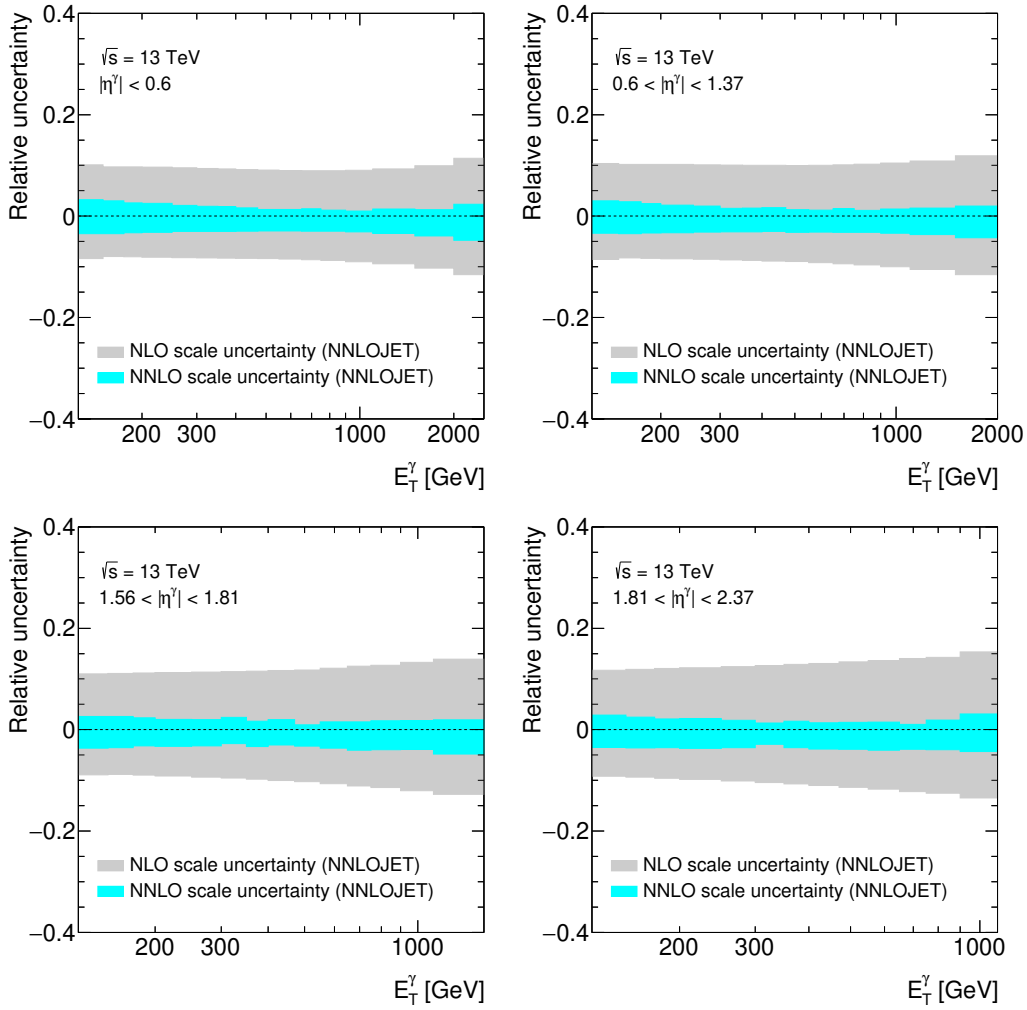

Figure 5: The relative theoretical uncertainty in the NNLOJET predictions arising from the scale variations as a function of E_{T}^{γ} in different regions of $|\eta^{\gamma}|$: for NLO QCD predictions (grey areas) and for NNLO QCD predictions (cyan areas).

Figures in paper

- **Results:**

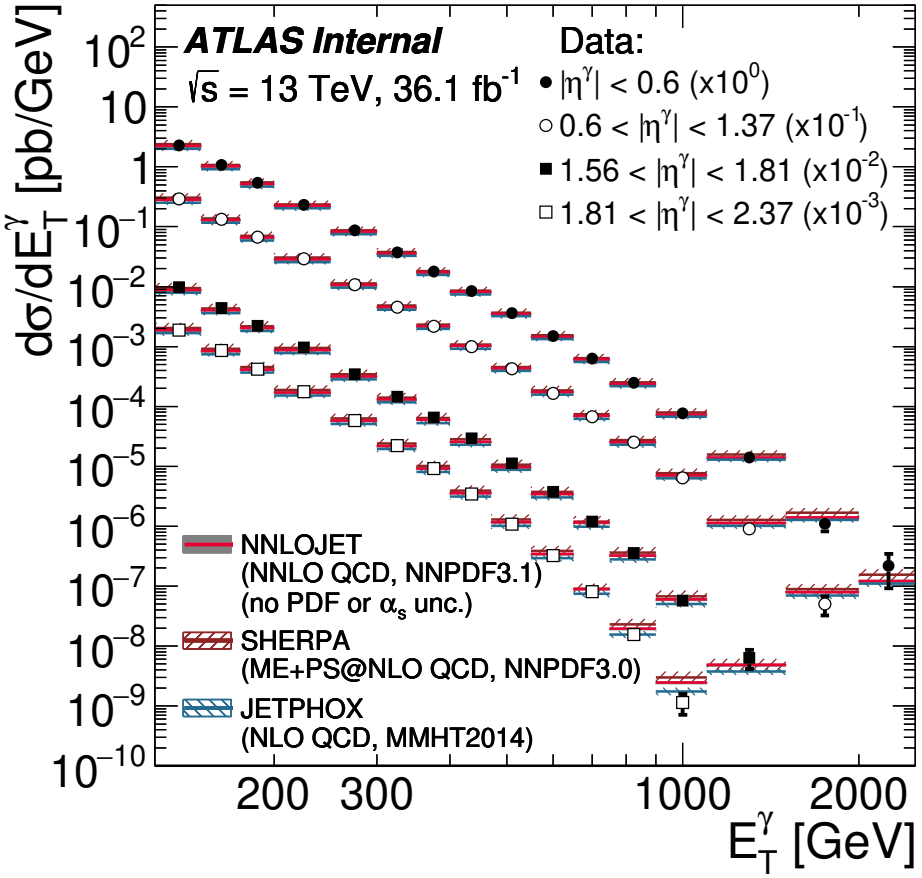

Figure 6: The measured differential cross section for isolated-photon production as a function of E_{T}^{γ} in $|\eta^{\gamma}| < 0.6$ (black dots), $0.6 < |\eta^{\gamma}| < 1.37$ (open circles), $1.56 < |\eta^{\gamma}| < 1.81$ (black squares) and $1.81 < |\eta^{\gamma}| < 2.37$ (open squares). The NLO pQCD predictions from JETPHOX, the ME+PS@NLO QCD predictions from SHERPA 2.2.2 and the NNLO QCD predictions from NNLOJET are also shown. The measurements and the predictions are normalised by the factors shown in parentheses to aid visibility. The error bars represent the data statistical uncertainties and systematic uncertainties added in quadrature. For most of the points, the error bars are smaller than the marker size and, thus, not visible. The bands represent the theoretical uncertainty associated to the predictions; in the case of NNLOJET, the uncertainties due to the PDFs and α_{s} are not included.

Figures in paper

- **Results:**

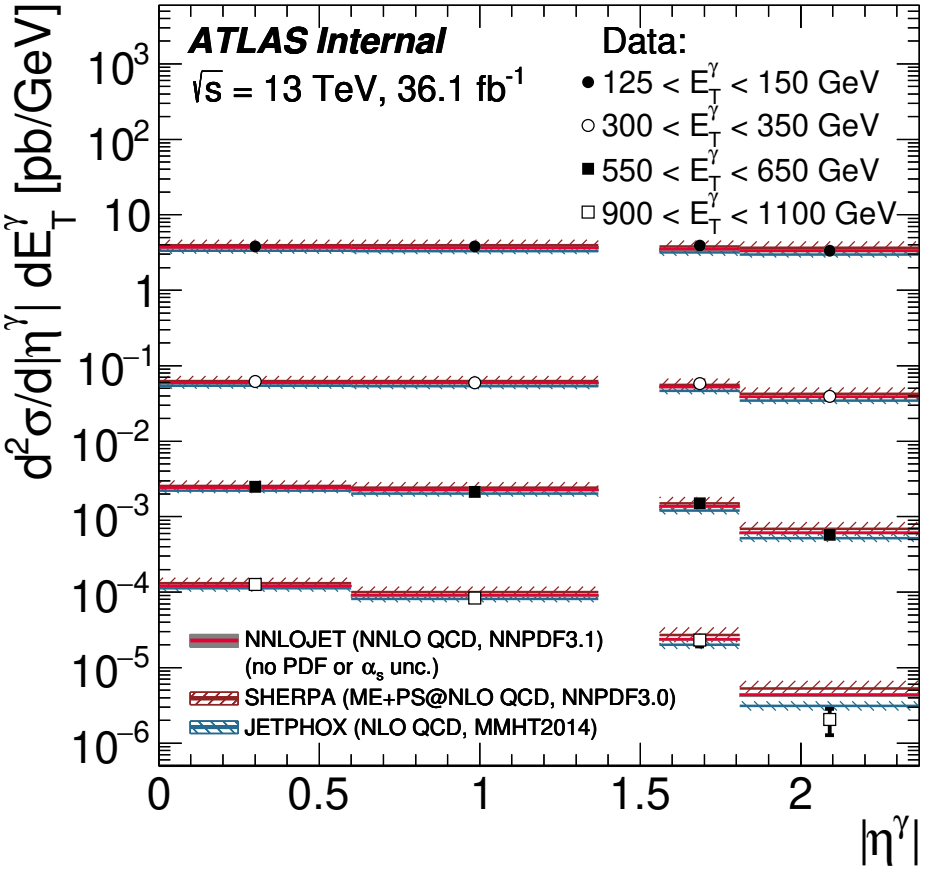

Figure 7: The measured double-differential cross section for isolated-photon production as a function of $|\eta^{\gamma}|$ in $125 < E_{\mathrm{T}}^{\gamma} < 150$ GeV (black dots), $300 < E_{\mathrm{T}}^{\gamma} < 350$ GeV (open circles), $550 < E_{\mathrm{T}}^{\gamma} < 650$ GeV (black squares) and $900 < E_{\mathrm{T}}^{\gamma} < 1100$ GeV (open squares). The NLO pQCD predictions from JETPHOX, the ME+PS@NLO QCD predictions from SHERPA 2.2.2 and the NNLO QCD predictions from NNLOJET are also shown. The measurements and the predictions are normalised by the factors shown in parentheses to aid visibility. The error bars represent the data statistical uncertainties and systematic uncertainties added in quadrature. For most of the points, the error bars are smaller than the marker size and, thus, not visible. The bands represent the theoretical uncertainty associated to the predictions; in the case of NNLOJET, the uncertainties due to the PDFs and α_{s} are not included.

Figures in paper

- **Results:**

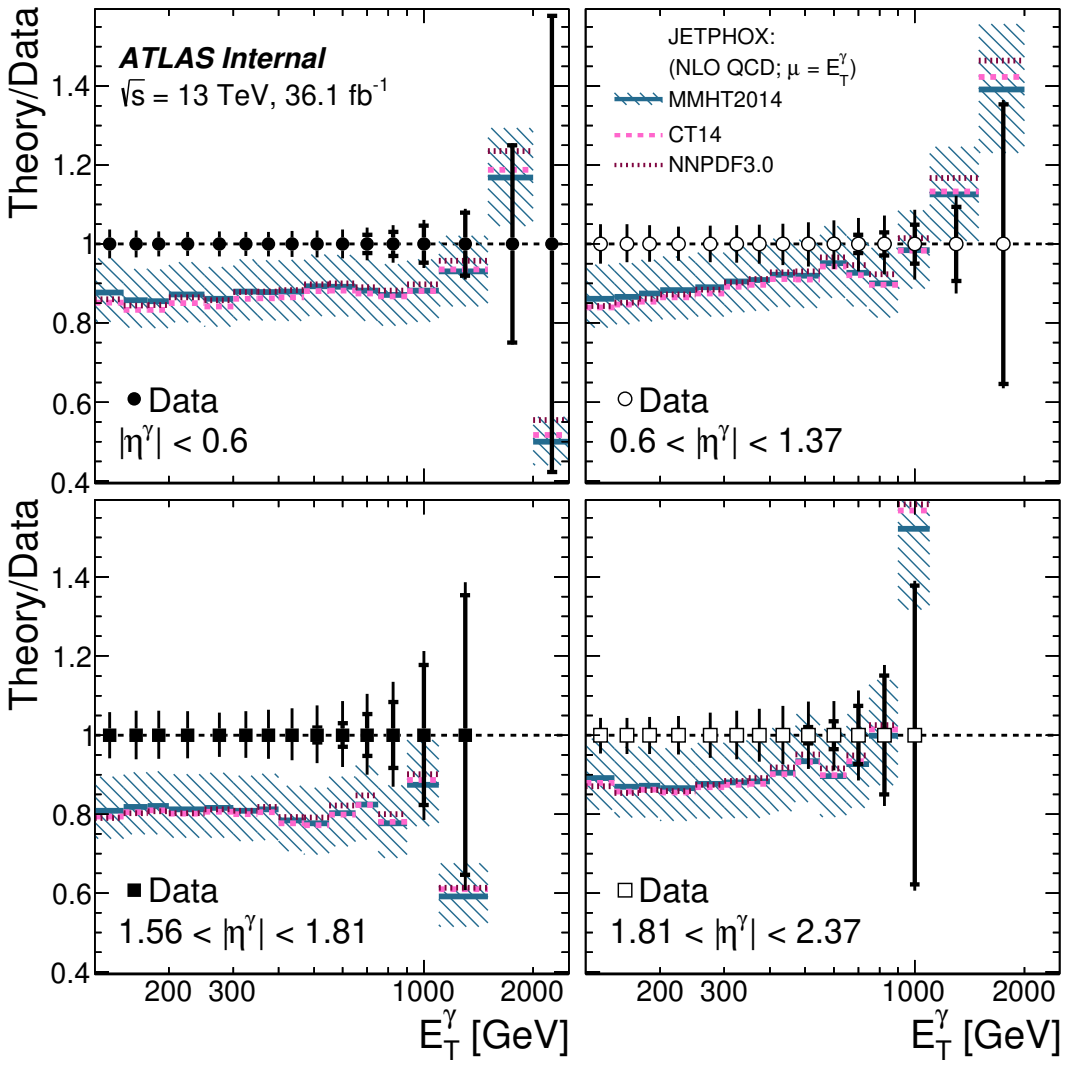

Figure 8: The ratio of the NLO pQCD prediction of JETPHOX with $\mu_R = \mu_F = \mu_f = E_T^\gamma$ using the MMHT2014 PDF set to the measured differential cross section for isolated-photon production (solid lines) as a function of E_T^γ in different regions of $|\eta^\gamma|$. The symbols for the data are centred at unity and the inner (outer) error bars represent the relative data statistical uncertainties (statistical and systematic uncertainties added in quadrature). The hatched bands represent the theoretical uncertainty. For comparison, the predictions using the CT14 (dashed lines) and NNPDF3.0 (dotted lines) PDF sets are also included.

Figures in paper

- **Results:**

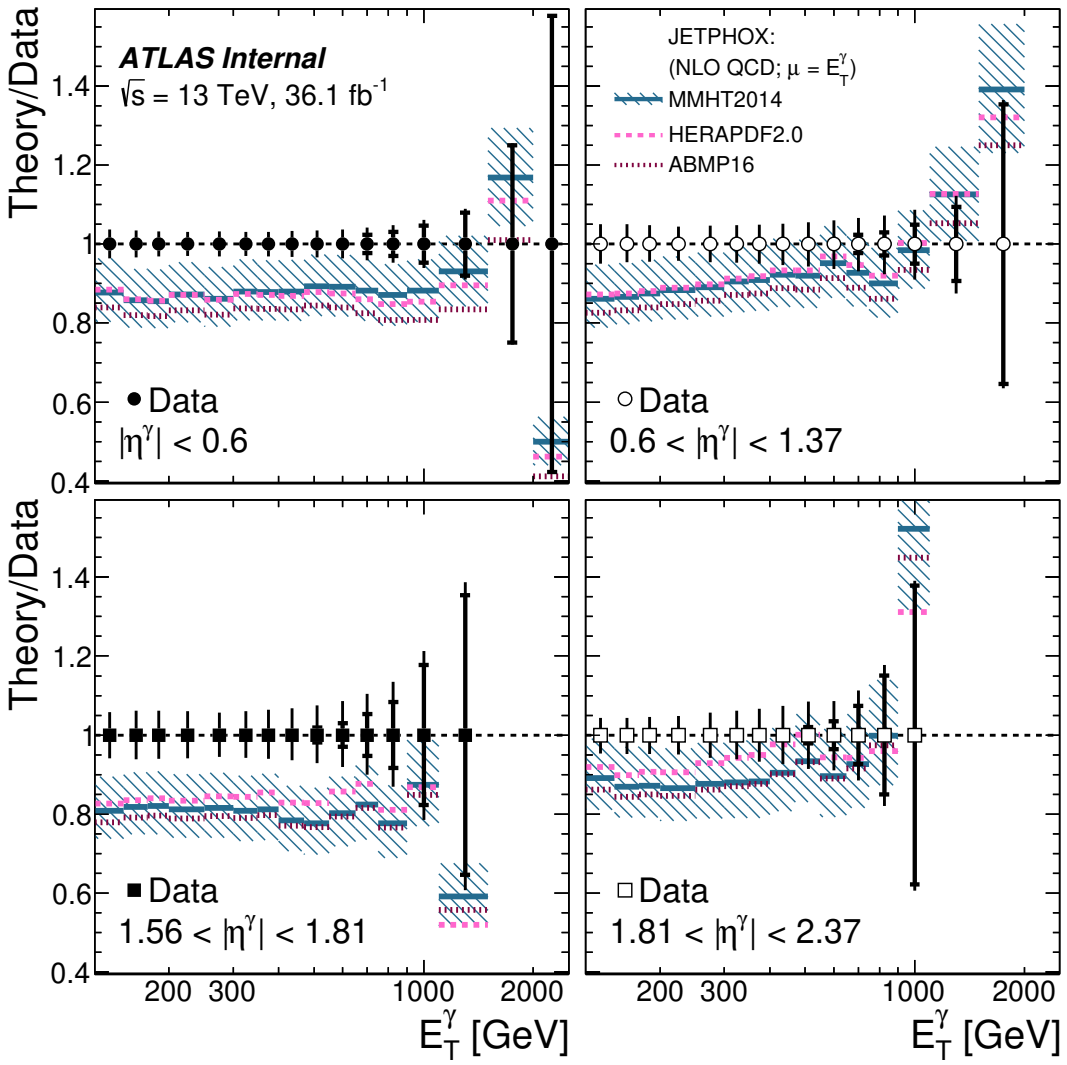

Figure 9: The ratio of the NLO pQCD prediction of JETPHOX with $\mu_R = \mu_F = \mu_f = E_T^\gamma$ using the MMHT2014 PDF set to the measured differential cross section for isolated-photon production (solid lines) as a function of E_T^γ in different regions of $|\eta^\gamma|$. The symbols for the data are centred at unity and the inner (outer) error bars represent the relative data statistical uncertainties (statistical and systematic uncertainties added in quadrature). The hatched bands represent the theoretical uncertainty. For comparison, the predictions using the HERAPDF2.0 (dashed lines) and ABMP16 (dotted lines) PDF sets are also included.

Figures in paper

- **Results:**

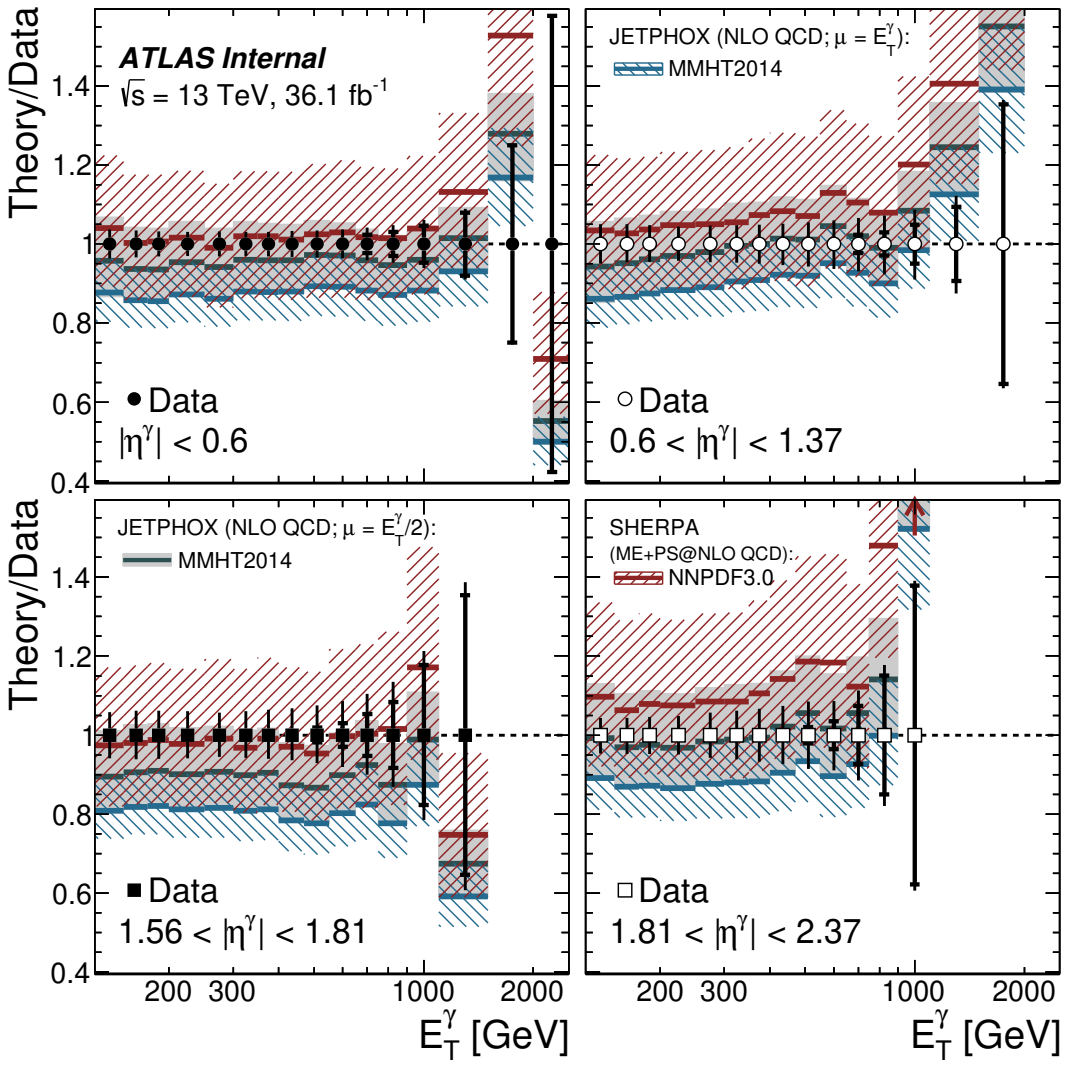

Figure 10: The ratio of the NLO pQCD prediction of JETPHOX with $\mu_R = \mu_F = \mu_f = E_T^\gamma$, the ratio of the NLO pQCD prediction of JETPHOX with $\mu_R = \mu_F = \mu_f = E_T^\gamma/2$ and the ratio of the ME+PS@NLO QCD prediction of SHERPA 2.2.2 to the measured differential cross section for isolated-photon production as a function of E_T^γ in different regions of $|\eta^\gamma|$. The symbols for the data are centred at unity and the inner (outer) error bars represent the relative data statistical uncertainties (statistical and systematic uncertainties added in quadrature). The bands represent the theoretical uncertainty.

Figures in paper

- **Results:**

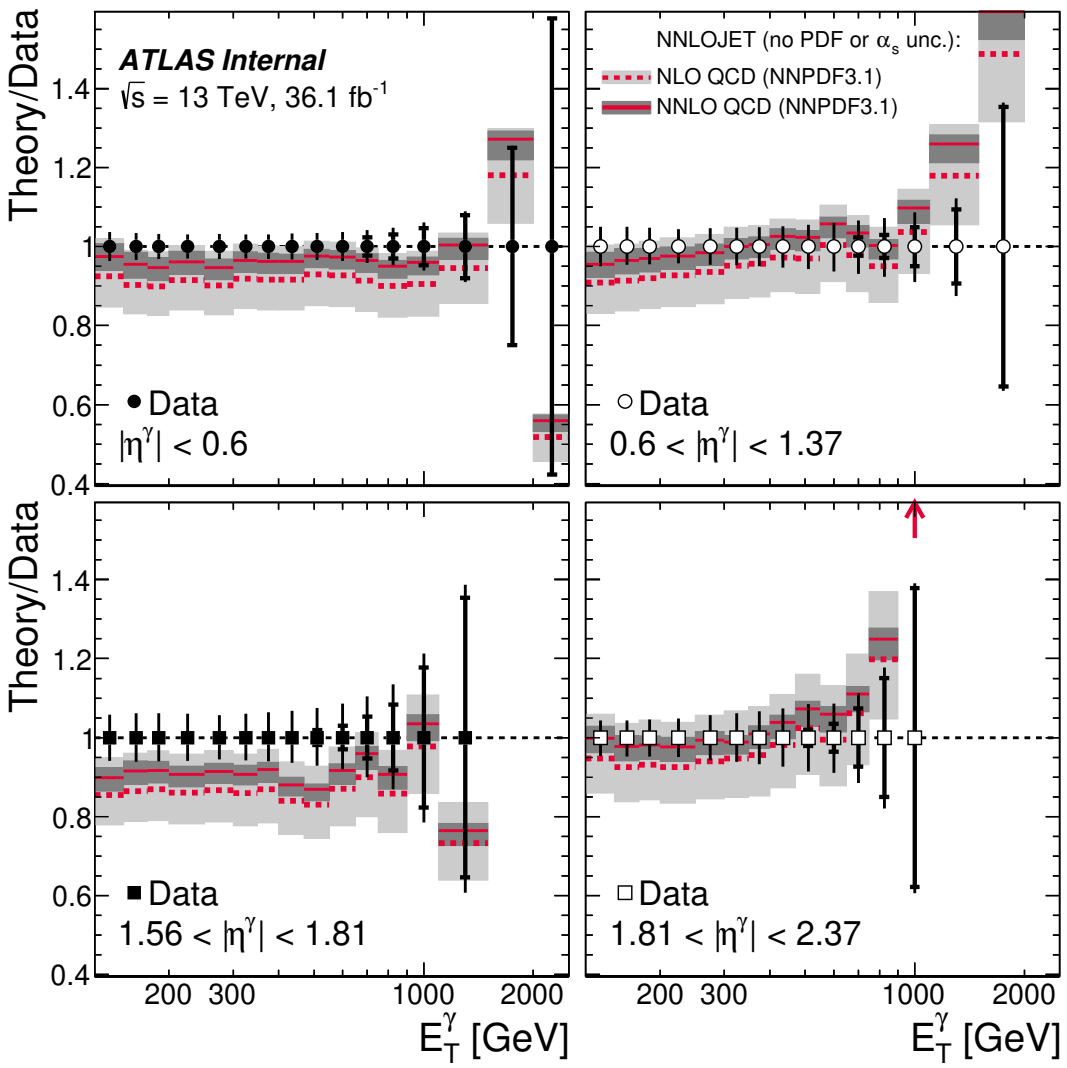

Figure 11: The ratio of the NNLO (NLO) QCD prediction of NNLOJET using the NNPDF3.1 PDF set to the measured differential cross section for isolated-photon production as a function of E_{T}^{γ} in different regions of $|\eta^{\gamma}|$ is shown as a solid (dashed) line. The symbols for the data are centred at unity and the inner (outer) error bars represent the relative data statistical uncertainties (statistical and systematic uncertainties added in quadrature). The shaded bands represent the theoretical uncertainties, which do not include the uncertainties due to the PDFs and α_{s}.

Figures in paper

- **Results:**

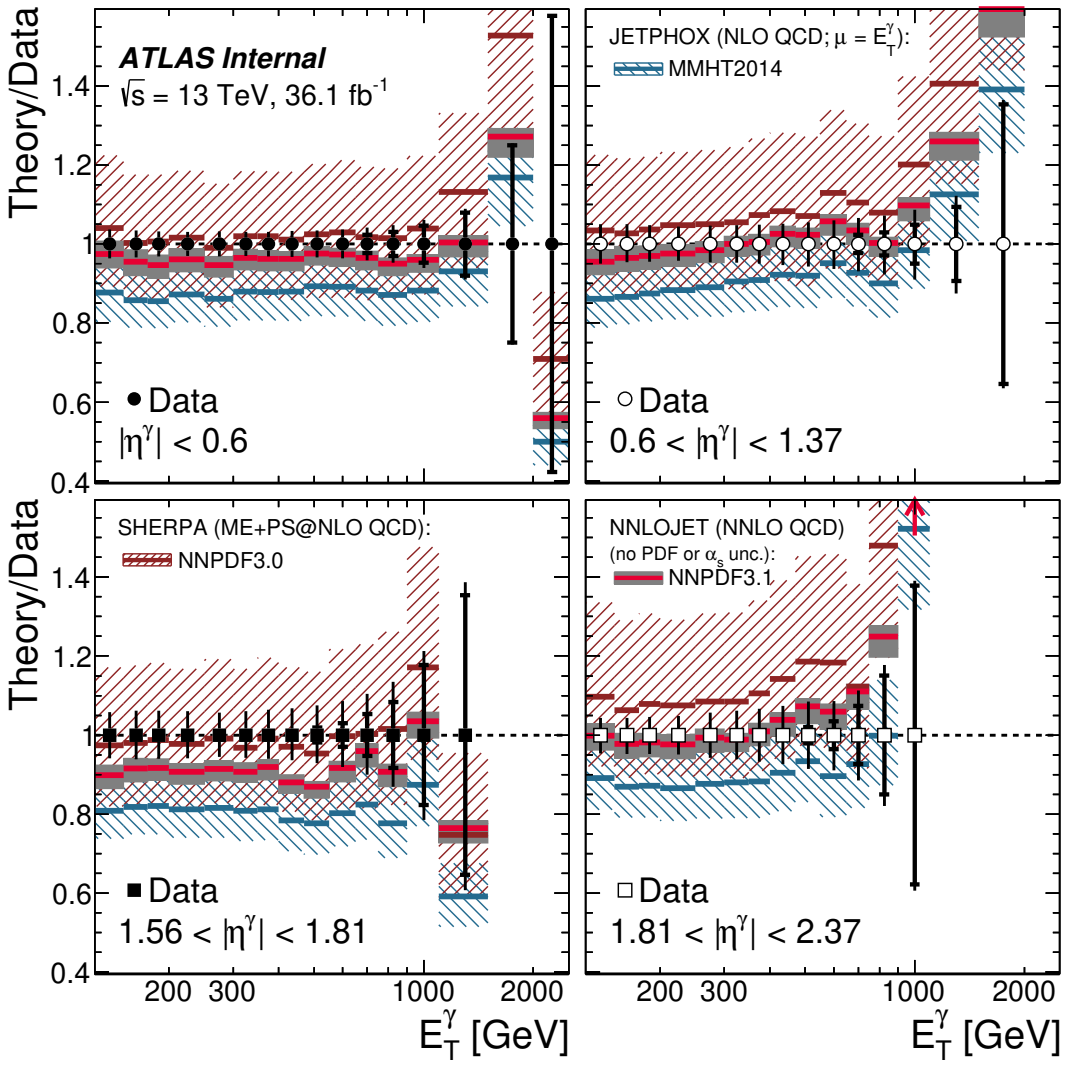

Figure 12: The ratio of the NLO pQCD prediction of JETPHOX with $\mu_R = \mu_F = \mu_f = E_T^\gamma$, the ratio of the ME+PS@NLO QCD prediction of SHERPA 2.2.2 and the ratio of the NNLO QCD prediction of NNLOJET to the measured differential cross section for isolated-photon production as a function of E_T^γ in different regions of $|\eta^\gamma|$. The symbols for the data are centred at unity and the inner (outer) error bars represent the relative data statistical uncertainties (statistical and systematic uncertainties added in quadrature). The bands represent the theoretical uncertainty; in the case of NNLOJET, the uncertainties due to the PDFs and α_s are not included.

Figures in auxiliary material

- **Experimental uncertainties:**

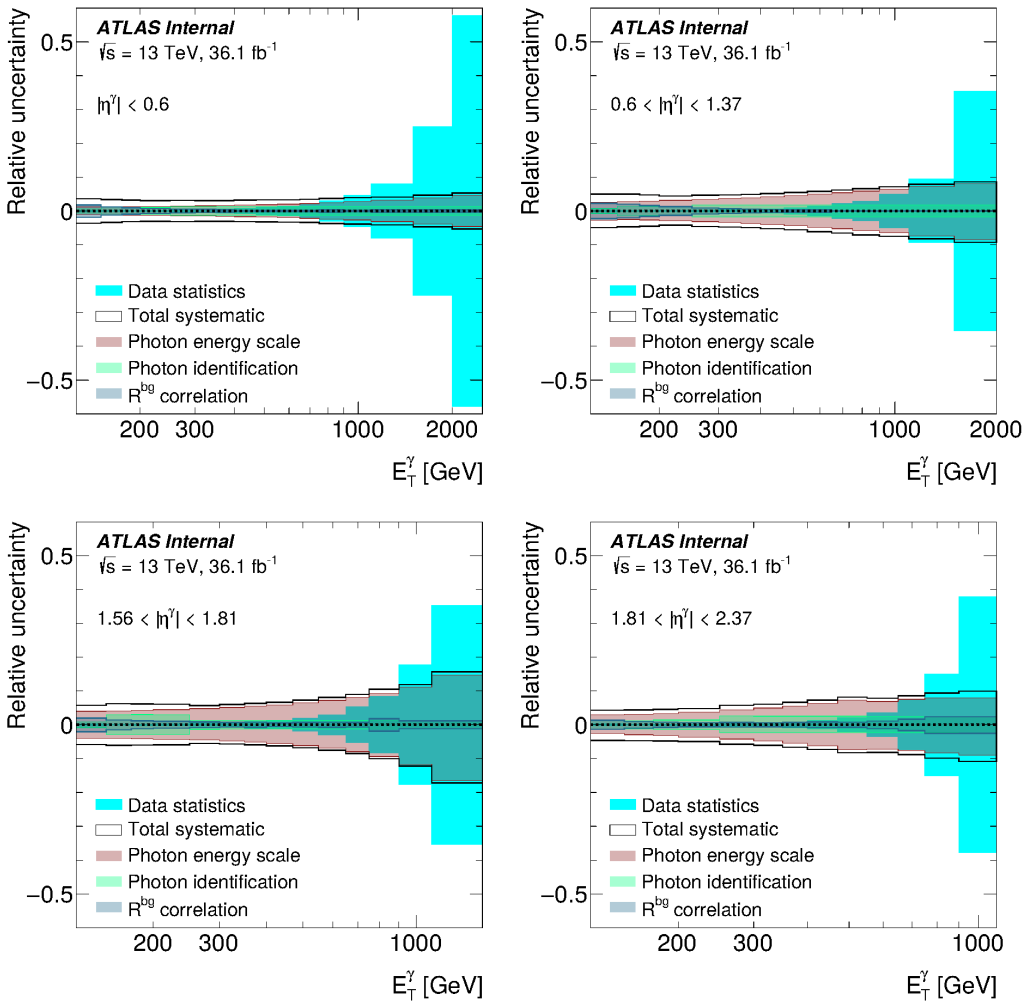

Figure 13: The relative total systematic uncertainty (white areas), the relative statistical uncertainty from the data (cyan areas), the relative uncertainty due to the photon energy scale (red areas), the relative uncertainty due to the photon identification efficiency (green areas) and the relative uncertainty due to R^{bg} (grey areas) as functions of E_{T}^{γ} in different $|\eta^{\gamma}|$ regions.

Figures in auxiliary material

- **Signal purity:**

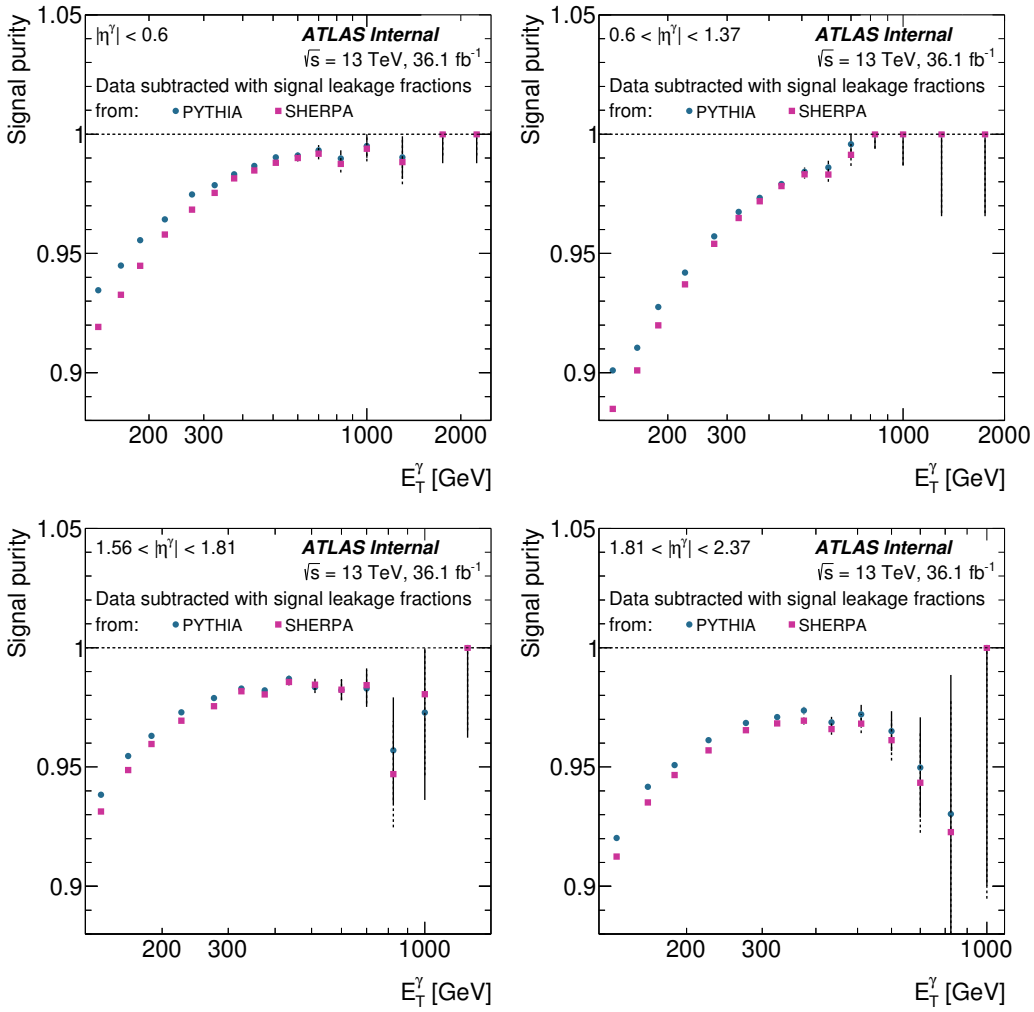

Figure 14: Estimated signal purities in data using signal leakage fractions from Pythia (dots) and Sherpa (squares) as functions of E_T^γ in different $|\eta^\gamma|$ regions.

Figures in auxiliary material

- **Results:**

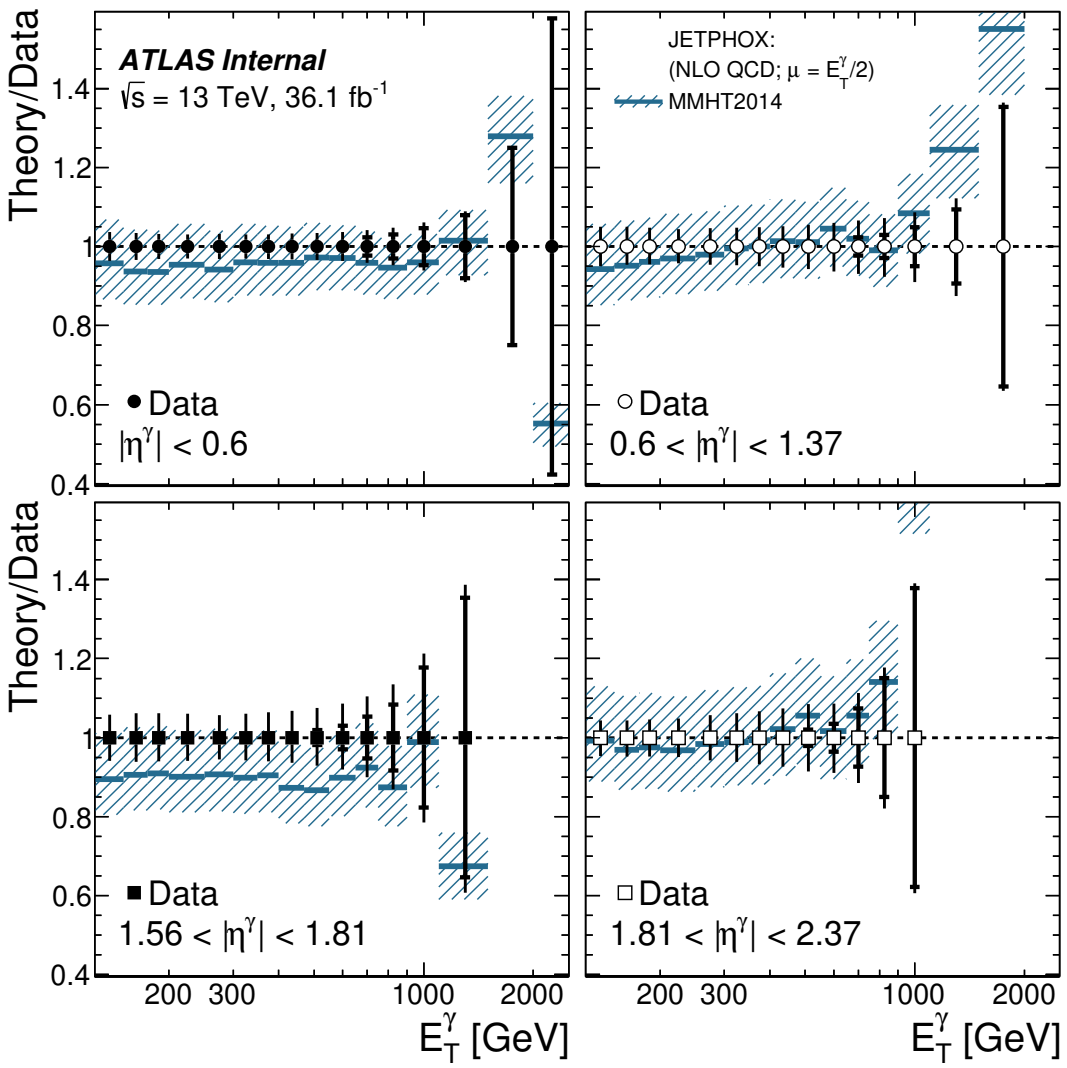

Figure 15: The ratio of the NLO pQCD prediction of JETPHOX with $\mu_R = \mu_F = \mu_f = E_T^\gamma/2$ using the MMHT2014 PDF set to the measured differential cross section for isolated-photon production (solid lines) as a function of E_T^γ in different regions of $|\eta^\gamma|$. The symbols for the data are centred at unity and the inner (outer) error bars represent the relative data statistical uncertainties (statistical and systematic uncertainties added in quadrature). The hatched bands represent the theoretical uncertainty.

Figures in auxiliary material

- **Results:**

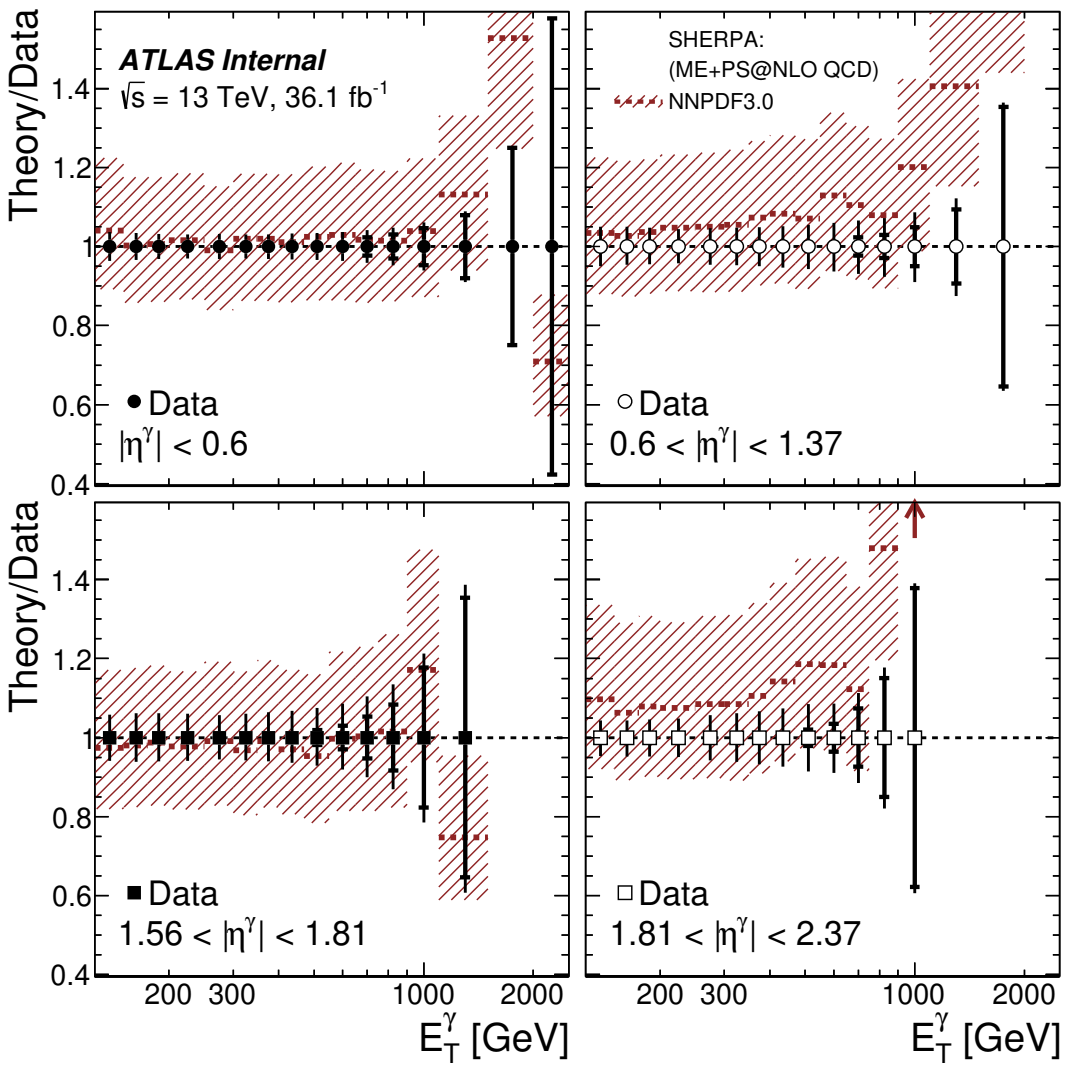

Figure 16: The ratio of the ME+PS@NLO QCD prediction of Sherpa 2.2.2 using the NNPDF3.0 PDF set to the measured differential cross section for isolated-photon production (dashed lines) as a function of E_{T}^{γ} in different regions of $|\eta^{\gamma}|$. The symbols for the data are centred at unity and the inner (outer) error bars represent the relative data statistical uncertainties (statistical and systematic uncertainties added in quadrature). The hatched bands represent the theoretical uncertainty.

Next steps of physics analysis

- **We have started the analysis of full Run 2 data using Release 21**

  → **control plots:**

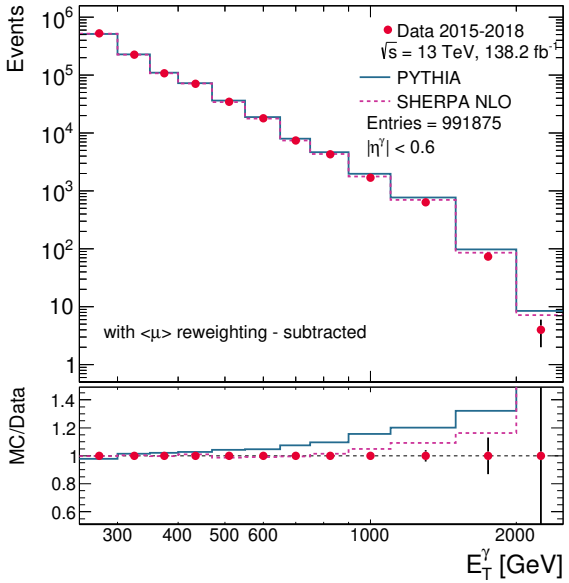

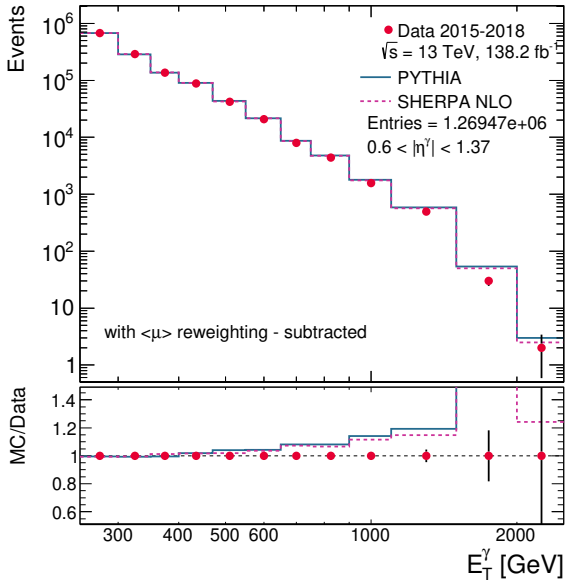

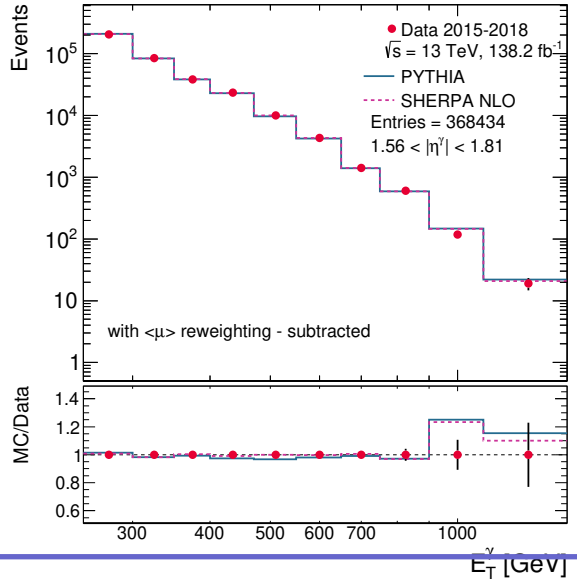

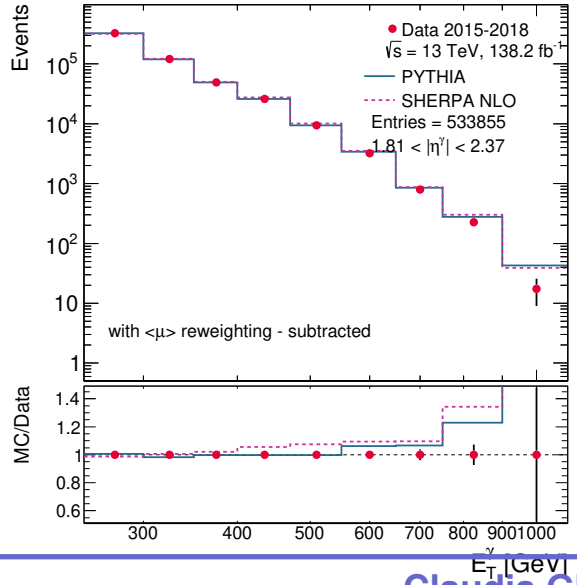

Next steps of physics analysis

- **We have started the analysis of full Run 2 data using Release 21**

  → **signal purity:**

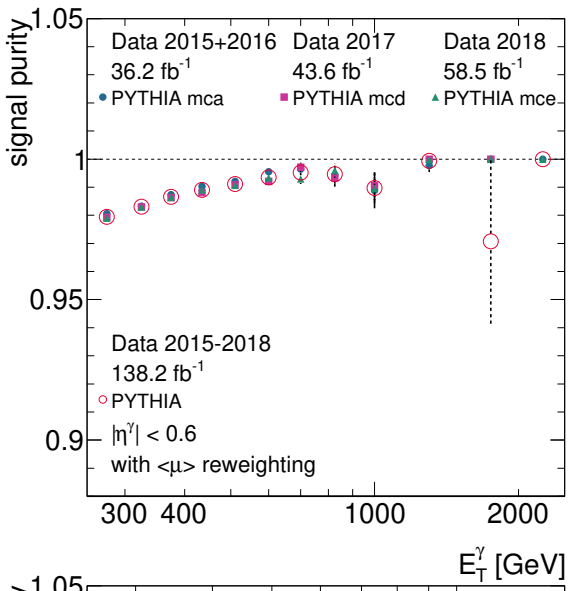

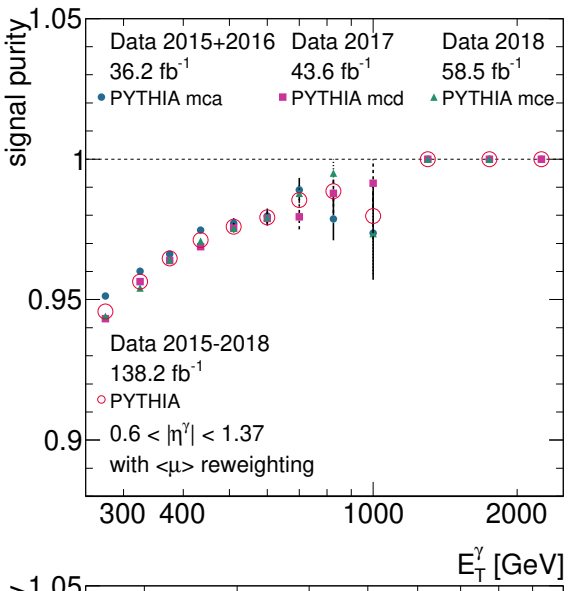

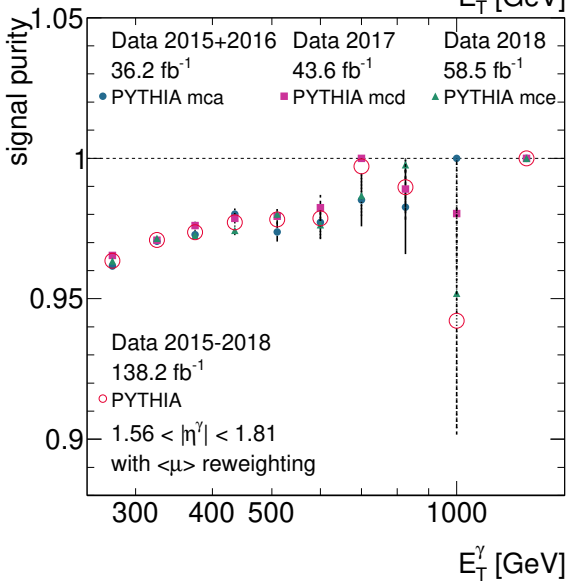

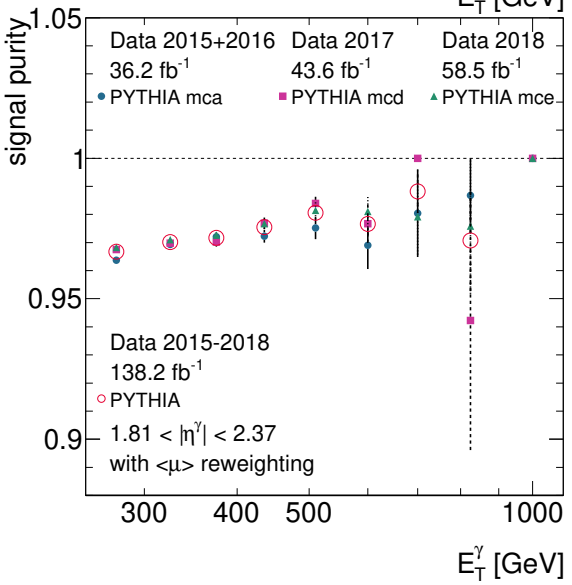

Next steps of physics analysis

- **We have started the analysis of full Run 2 data using Release 21**

  → **systematics:**

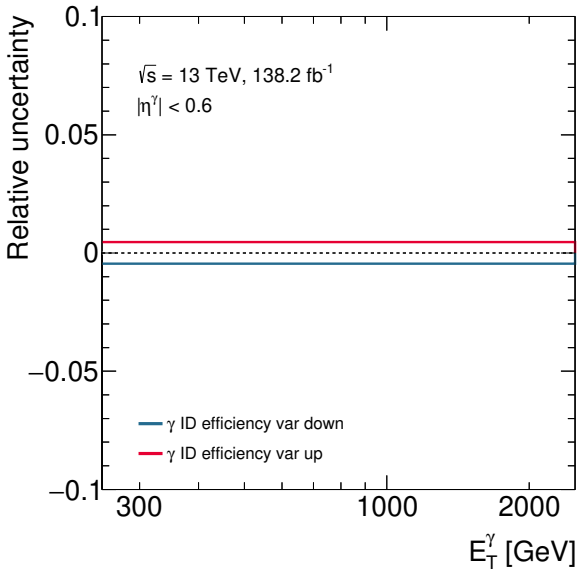

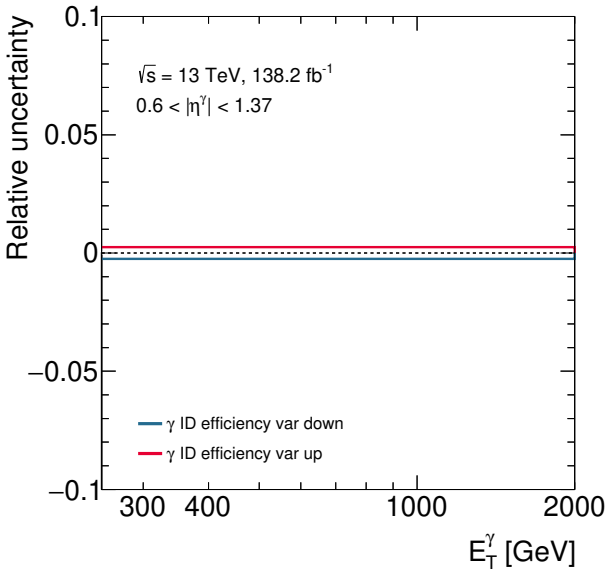

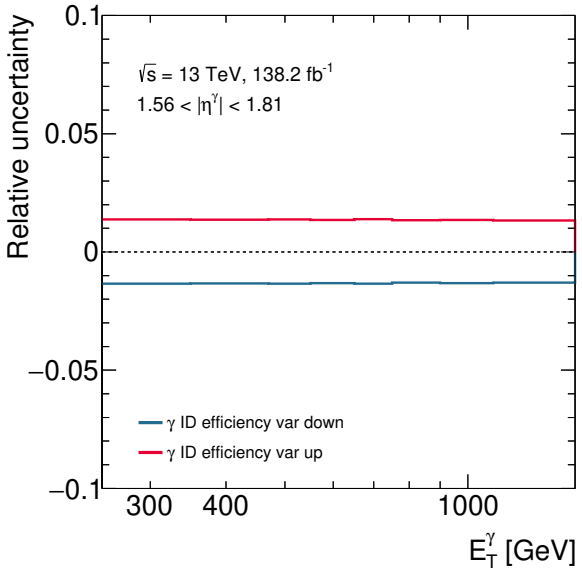

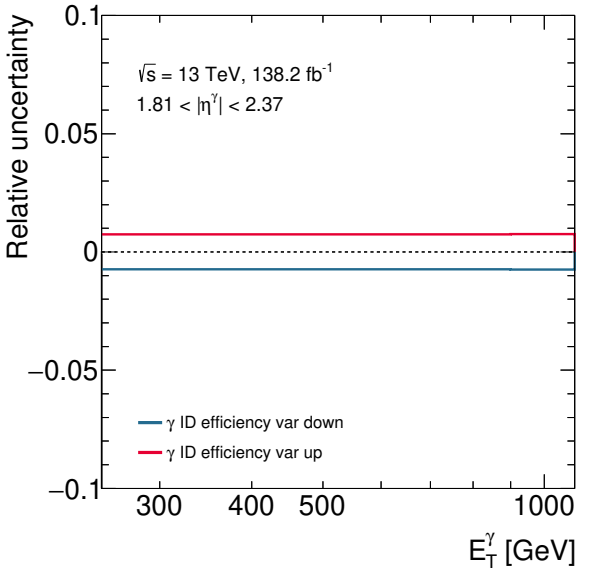

Next steps of physics analysis

- **We have started the analysis of full Run 2 data using Release 21**

  → **systematics:**

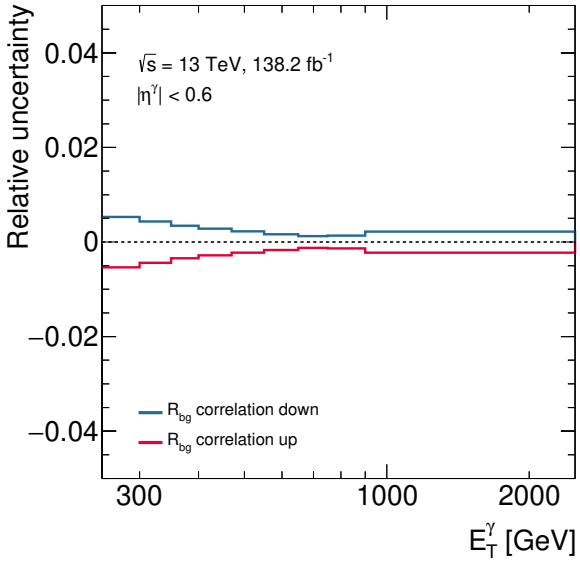

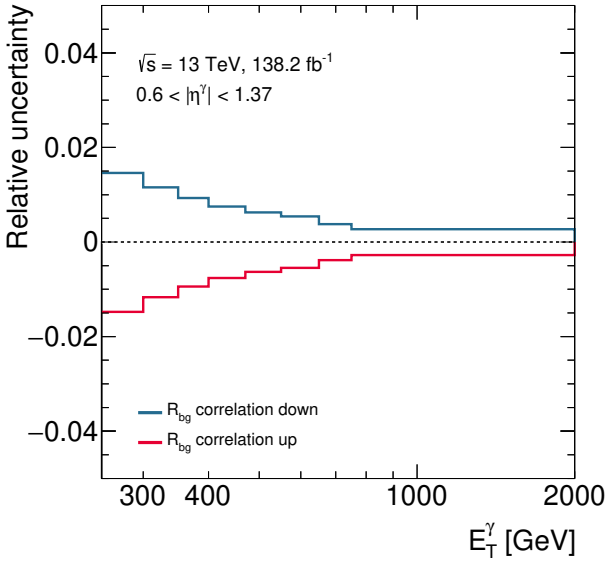

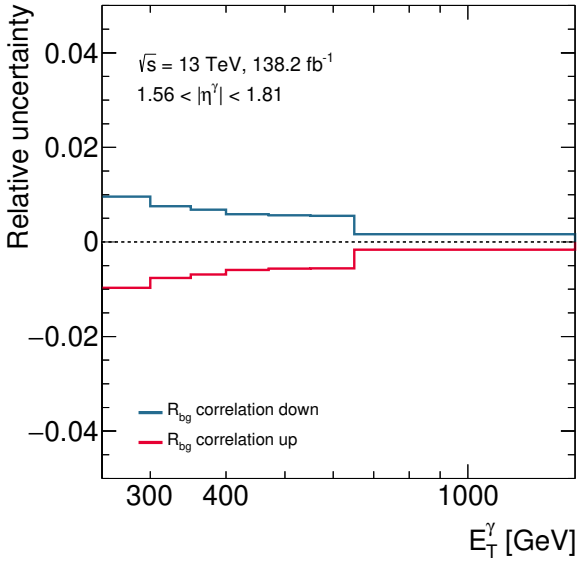

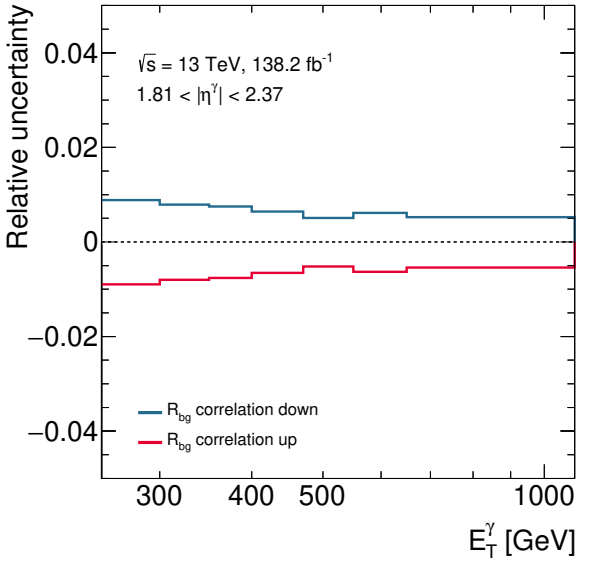

Next steps of physics analysis

- **We have started the analysis of full Run 2 data using Release 21**

  → **systematics:**

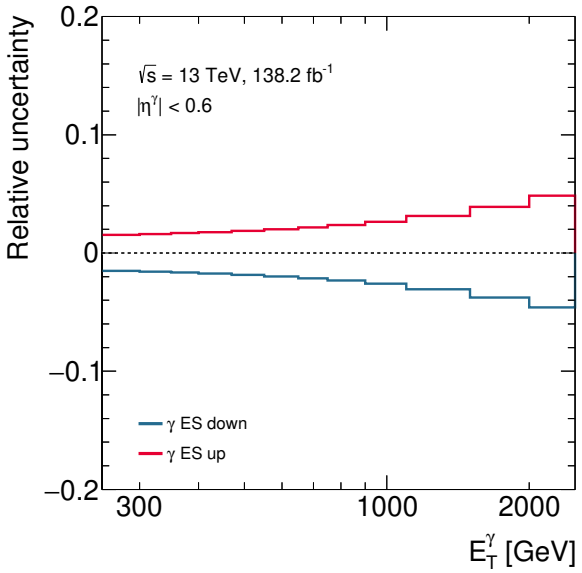

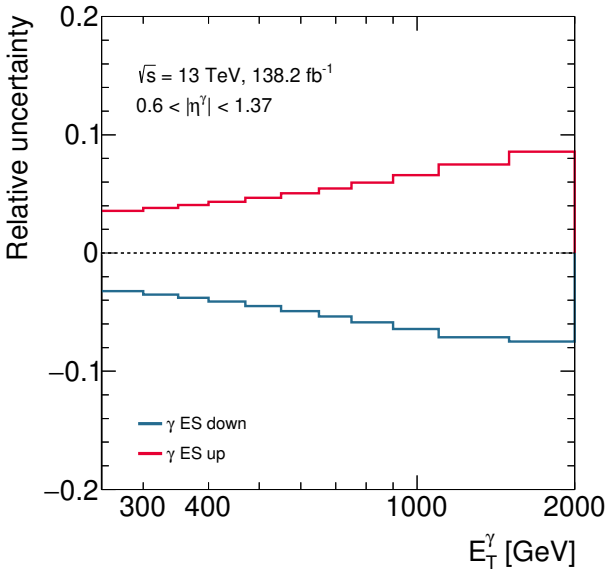

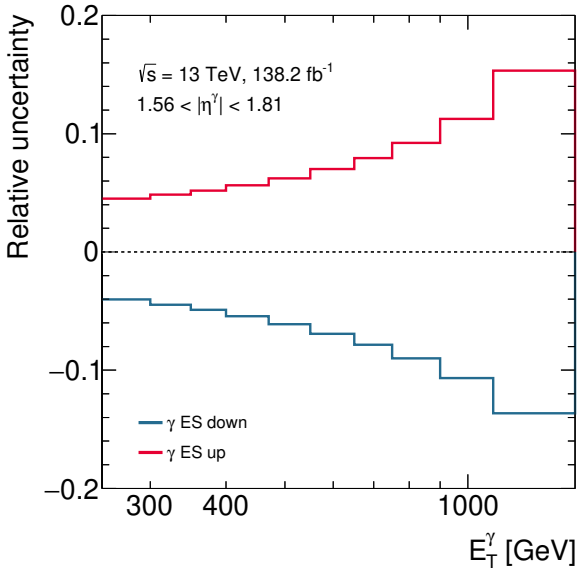

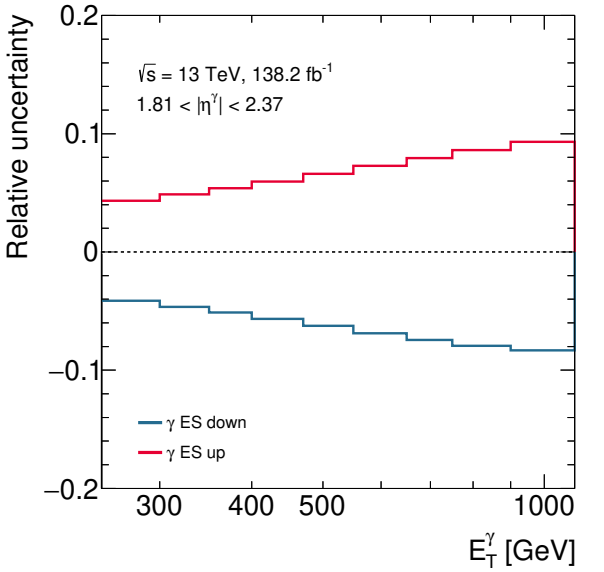

Summary and conclusions

- A measurement of the cross section for inclusive isolated-photon production in pp collisions at $\sqrt{s} = 13$ TeV using an integrated luminosity of 36.1 fb^{-1} of 2015+2016 data was presented
- Cross sections were measured as functions of E_{T}^{γ} in different regions of η^{γ} for $E_{\mathrm{T}}^{\gamma} > 125$ GeV, $|\eta^{\gamma}| < 2.37$ and $E_{\mathrm{T}}^{\mathrm{iso}} < 4.2 \cdot 10^{-3} \cdot E_{\mathrm{T}}^{\gamma} + 4.8\,\mathrm{GeV}$
- The E_{T}^{γ} reach was extended up to 2.5 TeV (1.5 TeV in previous measurements)
- The region where the measurements are dominated by systematic uncertainties is extended up to 1 TeV (0.6 TeV in previous measurements)
- Comparison with QCD predictions:
  - the NLO predictions are in agreement with the data within the experimental and theoretical uncertainties
  - the NNLO predictions are in excellent agreement with the data
  - differences observed between predictions based on different PDFs at high E_{T}^{γ}
  - these high precision measurements have the potential to constrain further the proton PDFs in future NNLO QCD fits, especially at high $E_{\mathrm{T}}^{\gamma} \leftrightarrow$ high x

Summary

- **Analysis with 2015+2016 data:**
  - → started in August 2017 and finished in March 2018 ($\approx$ 7 months)
  - → current status @ 15 months after finishing analysis:
    - → LE step before 2nd circulation

- **Analysis with 2015-2018 data:**
  - → started in June 2018
  - → current status:
    - → inclusive-photon measurements quite advanced
    - → paper will also include photon+jet production (not started)
    - → waiting for final photon and jet calibrations (estimated time: Summer)